ICON Documentation: Surface Albedo

Daniel Reinert

July 22, 2015

1 Surface albedo

Albedo is defined as the ratio of upwelling to downwelling radiative flux at the surface. The downwelling flux may be written as the sum of a direct and a diffuse component. Thus, two different albedos based on either the diffuse or direct flux component can be defined. White-sky albedo is defined as albedo in the absence of a direct component when the diffuse component is isotropic. Black sky albedo is defined as albedo in the absence of a diffuse component. While black sky albedo is a function of the solar zenith angle, white sky albedo is essentially zenith angle independent.

In the shortwave radiation scheme, the reflection at the surface is handled considering both direct and diffuse downward radiation fluxes. For this, spectral albedos for parallel and diffuse radiation are needed. The spectral albedos distinguish between the visible ($0.3 - 0.7\,\mu$m) and near-infrared ($0.7 - 5.0\,\mu$m) spectral bands. Thus, 4 albedo values ($\alpha^{vis}_{\text{dir}}$, $\alpha^{nir}_{\text{dir}}$, $\alpha^{vis}_{\text{diff}}$, $\alpha^{nir}_{\text{diff}}$) are required for each grid point. The indices `dir` and `diff` indicate the type of radiation (direct or diffuse), whereas the indices `vis` and `nir` distinguish the spectral bands (UV-visible or near-infrared). In the following we will separately discuss snow-free and snow-covered land, open water, sea-ice and fresh water lake points.

1.1 Albedo for diffuse downward radiation (white sky)

1.1.1 Snow-free land points

Over snow-free land, white sky surface albedos ($\alpha^{vis}_{\text{diff}}$, $\alpha^{nir}_{\text{diff}}$) are derived from monthly mean climatologies build from 16-days MODIS albedo over the year 2000-2003 (Schaaf *et al.*, 2002). Separate datasets are available for UV-visible and near-infrared spectral bands. The model does a linear interpolation between successive months, assuming that the monthly field belongs to the 15th of the month. The values are updated on a daily basis. If land tiles are used, the same MODIS albedo is assigned to every land tile of a single grid cell.

1.1.2 Snow-covered land points

The snow albedo for visible and near-infrared spectral bands is calculated by

$$\alpha^{vis}_{\text{diff}} = \alpha^{nir}_{\text{diff}} = \alpha_{s,min} + S_{age}\,(\alpha_{s,max} - \alpha_{s,min})\,. \tag{1}$$

with $\alpha_{s,max}$ and $\alpha_{s,min}$ denoting the upper and lower limits and S_{age} denoting a snow ageing factor (to be described lateron). $\alpha_{s,min}$ is landuse class specific with lower values for forest than for grassland or bare areas. Generally it is set to 60 % of the tabulated landuse class specific maximum snow albedo. The valid range is $0.2 \leq \alpha_{s,min} \leq 0.5$. For glaciers, a temperature dependency is assumed for $\alpha_{s,min}$, i.e. the minimum albedo is assumed to be lower the warmer the surface is.

$$\alpha_{s,min} = (1-\gamma)\cdot 0.5 + \gamma \cdot 0.7\,, \tag{2}$$

with

$$\gamma = \min(1, \frac{T_0 - T_{\text{snow}}}{10}) \,, \tag{3}$$

with T_0 the ice melting temperature. Note that $T_{\text{snow}} \geq T_0$.

Similar to $\alpha_{s,min}$, a landuse class dependent $\alpha_{s,max}$ is assumed as well.

$$\alpha_{s,max} = \min \left[\alpha_{s,max}^{ilu}, \alpha_{s,max}^{ilu,LIM} \cdot \min \left(1, \sqrt{0.25 + \frac{0.25 \, \max(0.05, h_{snow})}{\max(\min(0.5, z_0^{ilu}), 10^{-3} \sigma_{SSO})}} \right) \right] \tag{4}$$

According to equation 4 the landuse dependent maximum snow albedo $\alpha_{s,max}^{ilu}$ is further limited in case of thin snow cover depending on landuse roughness length z_0^{ilu} and SSO standard deviation σ_{SSO}. It is assumed that non-forest vegetation is fully covered by snow if the snow depth exceeds three times the roughness length. The snow depth is taken to be at least 5 cm here because the effect of partial snow cover is considered in equation 12.

It is well known that snow albedo decreases with increasing snow age due to various meteorological and environmental factors. This is taken into account by a snow ageing function $0 \leq S_{\text{age}} \leq 1$ which is 1 for fresh snow and approaches 0 for old snow. S_{age} is computed as follows:

$$S_{\text{age}}^{n+1} = S_{\text{age}}^{n} + \Delta t \, \frac{\partial S_{\text{age}}^{+}}{\partial t} - \Delta t \, \frac{\partial S_{\text{age}}^{-}}{\partial t} \tag{5}$$

$\partial S_{\text{age}}^{+}/\partial t$ and $\partial S_{\text{age}}^{-}/\partial t$ denote refresh and decay rates, respectively. The refrefresh rate is parameterized as follows:

$$\frac{\partial S_{\text{age}}^{+}}{\partial t} = R_{\text{snow}} \left[0.1 + \max \left(0.1, 0.02 \left(T_0 - T \right) \right) \right] \,, \tag{6}$$

with the snowfall rate R_{snow}, the freezing temperature T_0 and the air temperature of the lowest model level T. The refresh rate is linear in time and becomes $1/day$ for a temperature-dependent snow fall rate between $10\,\text{kg/m}^2$ per day at freezing point and $5\,\text{kg/m}^2$ per day for temperatures below $-5°\text{C}$.

For the decay rate it is assumed:

$$\frac{\partial S_{\text{age}}^{-}}{\partial t} = \left[\frac{1}{\tau_{\text{snow}}} + 0.1 \cdot R_{\text{rain}} \right] S_{\text{age}}^{n} \tag{7}$$

It is the sum of an inverse background ageing time scale τ_{snow} and a factor dependent on the rainfall rate R_{rain} multiplied by the snow age itself, making the decay exponential. For $S_{\text{age}}^{n} = 1$ the rainfall decay rate becomes $1/day$ at a rainfall rate of $10\,\text{kg/m}^2$ per day.

The ageing time scale τ_{snow} is assumed to be the minimum of two ageing time scales τ_{snow}^{1} and τ_{snow}^{2}, which take into account distinct ways of snow ageing:

$$\tau_{\text{snow}} = \min \left(\tau_{1,\text{snow}}, \tau_{2,\text{snow}} \right) \tag{8}$$

$\tau_{1,\text{snow}}$ is temperature dependent and is parameterized as follows:

$$\tau_{1,\text{snow}} = 86400 \cdot \min \left[28.0, 2.0 + 1.733 \cdot (T_0 - \min(T_0, T_{\text{snow}})) \right] \tag{9}$$

It increases from 2 days at freezing point up to 28 days below $-15°\text{C}$.

The second ageing time scale $\tau_{2,\text{snow}}$ takes into account the effect of wind speed on snow ageing (blowing snow).

$$\tau_{2,\text{snow}} = \max \left(86400, \frac{2.0E8 \cdot \max(0.05, h_{\text{snow}})}{\min(300, u_{10m}^2 + v_{10m}^2 + 12)} \right) \tag{10}$$

Thin snow cover tends to get broken under strong winds, which reduces the area averaged albedo. An offset is added in order to ensure moderate aging for low snow depths.

In the case of falling snow the decay rate is decremented by the refresh rate, mimicing that the decay should be largely stopped, if a new layer of fresh snow is added.

$$\frac{\partial S^{-}_{\text{age}}}{\partial t} = \left(\frac{1}{S^{n}_{\text{age}}} \frac{\partial S^{-}_{\text{age}}}{\partial t} - \frac{\partial S^{+}_{\text{age}}}{\partial t} \right) S^{n}_{\text{age}} \tag{11}$$

The reason for multiplying the refresh rate with S^{n}_{age} is not clear, however it is expected to have negligible impact on the results.

1.1.3 Partial snow cover

If there is little snow and/or high vegetation, it is assumed that only part of the grid cell is covered by snow. The amount of snow coverage is represented in terms of a snow fraction F_{snow}, which is the ratio of the snow covered area to the total grid cell area. If $F_{snow} < 1$, the albedo is given as a weighted average of the snow-covered and snow-free values.

$$\alpha^{\lambda}_{\text{diff}} = F_{\text{snow}}\, \alpha_{s,\text{diff}} + (1 - F_{\text{snow}})\, \alpha_{\text{diff}} \tag{12}$$

λ designates the spectral wavelength band.

1.1.4 Open-water points

For open-water points, the white sky albedos are set to a constant value.

$$\alpha^{\lambda}_{\text{diff}} = 0.07$$

1.1.5 Sea-ice points

The ice surface albedo for diffuse radiation is approximated as:

$$\alpha^{\lambda}_{\text{diff}} = \alpha_{i,max} - (\alpha_{i,max} - \alpha_{i,min}) \exp\left[-C_{\alpha} \left(\frac{T_{f0} - T_i}{T_0} \right) \right], \tag{13}$$

where $\alpha_{i,max} = 0.7$ and $\alpha_{i,min} = 0.43$ are maximum and minimum values of the sea-ice albedo, $T_0 = 273.15\,\text{K}$ is the fresh water freezing point, T_i is the ice surface temperature and $C_{\alpha} = 95.6$ is a fitting coefficient. Equation 13 is meant to implicitly account (in a crude way) for the seasonal changes of α. The ice albedo is the lower the warmer, and therefore wetter the ice is.

1.1.6 Fresh water lake points

For frozen lakes, equation 13 is used, too. However, the maximum and minimum ice albedo is set to $\alpha_{i,max} = 0.6$ and $\alpha_{i,min} = 0.1$, respectively. If no ice is present, the surface albedo for diffuse radiation is approximated as

$$\alpha^{\lambda}_{\text{diff}} = 0.07$$

1.1.7 Sample plots

Figure 1 and 2 show the diffuse surface albedo (UV-visible and near-infrared) for the 1st June 2012 00UTC as it is operationally used by ICON for snow-free land points. Note that compared to the original MODIS data, the Saharan diffuse albedo has been slightly reduced in order to compensate for a model cold bias in that region.

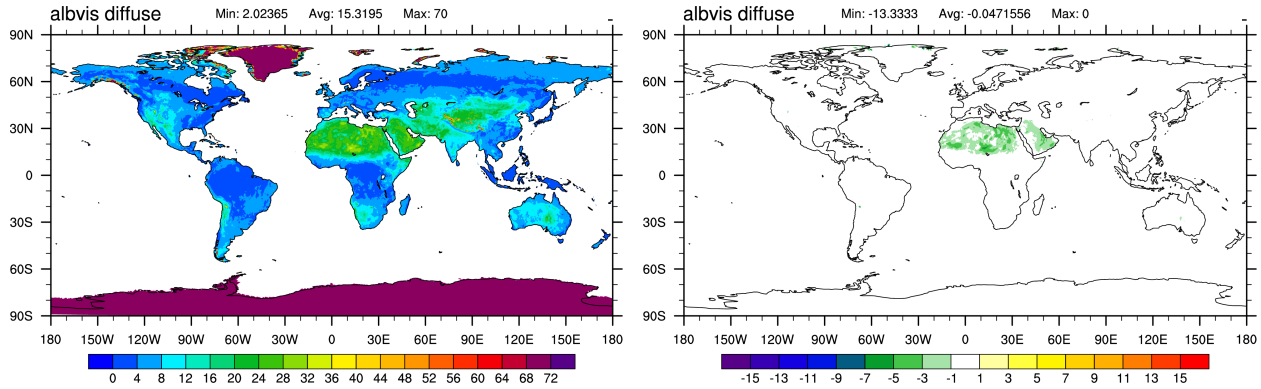

Figure 1: White sky (diffuse) albedo for UV-visible (left) spectral bands for the 1st June 2012 00UTC and its deviation from the original MODIS values (actual-original).

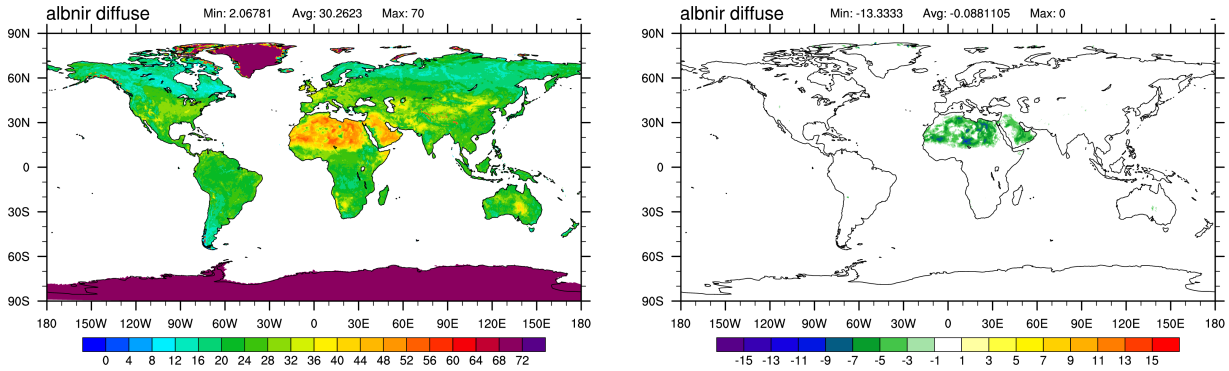

Figure 2: White sky (diffuse) albedo for near-infrared spectral bands (left) for the 1st June 2012 00UTC and its deviation from the original MODIS values (actual-original).

1.2 Albedo for direct downward radiation (black sky)

While the diffuse albedo does not depend on the solar zenith angle (SZA) θ_0, direct albedo does (Yang *et al.*, 2008). Up to ICON-NWP version 2.0.05 the formula for taking into account the zenith angle dependency was adapted from the Ritter-Geleyn radiation scheme. It was applied irrespective of the underlying surface type.

$$\alpha^{\lambda}_{\mathrm{dir}} = \frac{1.0 + 0.5\,\cos(\theta_0)\left(\frac{1}{\alpha^{\lambda}_{\mathrm{diff}}} - 1\right)}{\left[1.0 + \cos(\theta_0)\left(\frac{1}{\alpha^{\lambda}_{\mathrm{diff}}} - 1\right)\right]^2} \tag{14}$$

This parameterization was applied for both the UV-visible and near-infrared spectral bands. The functional dependency is visualized in Figure 3 for three different values of the diffuse albedo. At large solar zenith angles the direct albedo approaches 100 % irrespective of the diffuse albedo - a feature which is not supported by measurements. Further note that the solar zenith angle at which $\alpha^{\lambda}_{\mathrm{dir}} = \alpha^{\lambda}_{\mathrm{diff}}$ decreases with increasing $\alpha^{\lambda}_{\mathrm{diff}}$. As far as we know this is not supported by albedo measurements.

From ICON-NWP version 2.0.06 on, the parameterization 14 is retained for water and ice points only. For snow-free land points a formulation following Briegleb and Ramanathan (1982) is used.

$$\alpha^{\lambda}_{\mathrm{dir}} = \alpha^{\lambda}_{\mathrm{diff}}\,\frac{1.0 + d}{1.0 + 2.0d\cos(\theta_0)} \tag{15}$$

d is a tuning constant taking into account that albedo can have a stronger or weaker dependence on SZA, depending on the surface type. In ICON we set

$$d = \begin{cases} 0.4 & \text{if } z_0 \leq 0.15\,\mathrm{m} \\ 0.1 & \text{if } z_0 > 0.15\,\mathrm{m}\,, \end{cases} \tag{16}$$

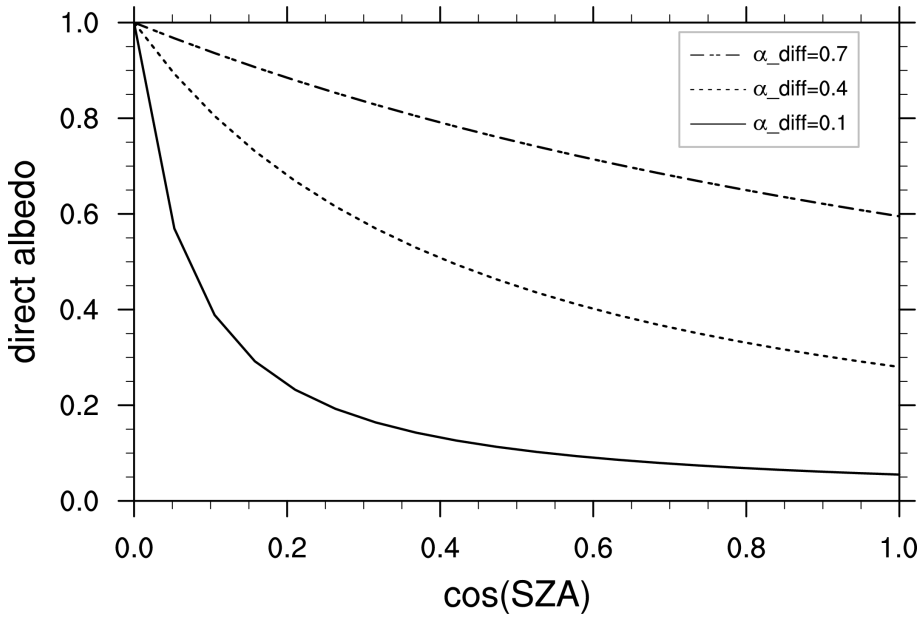

Figure 3: Solar zenith angle (SZA) dependence of the Black-sky (direct) albedo following Ritter (pers. comm.). Different lines show functional the dependency for 3 different values of the diffuse albedo. Note that the direct albedo always reaches 1 at $\theta_0 = 90°$ zenith angle irrespective of the diffuse albedo.

meaning that a strong dependence on SZA is assumed for bare soil and low vegetation, while a weaker dependence is assumed for high vegetation (e.g. forests). The functional dependency is depicted in Figure 4. Unlike the Ritter-Paratemerization, Briegleb and Ramanathan (1982) assume $\alpha^{\lambda}_{\text{dir}}(60°) = \alpha^{\lambda}_{\text{diff}}$, which can easily be seen by inserting $\theta_0 = 60°$ into equation 15. This assumption is not too bad, but still only approximately true.

For snow-covered land points, we make use of modified Ritter-parameterization as proposed by Zängl (pers. comm.). Basically, the direct albedo is not allowed to exceed the diffuse albedo in cases with rough vegetation and/or mountainous regions. The direct albedo is estimated as follows:

$$\alpha^{\lambda}_{\text{dir}} = \min\left[\alpha_{\text{dir}^{\lambda}}, \alpha^{\text{LIM}}_{\text{dir}}\right] \tag{17}$$

I.e. the direct albedo computed according to equation (14) is not allowed to exceed the limit $\alpha^{\text{LIM}}_{\text{dir}}$. The latter is defined as a weighted average of the unlimited direct albedo $\alpha^{\lambda}_{\text{dir}}$ and the diffuse albedo $\alpha^{\lambda}_{\text{diff}}$.

$$\alpha^{\text{LIM}}_{\text{dir}} = \gamma \cdot \alpha^{\lambda}_{\text{diff}} + (1 - \gamma) \cdot \alpha^{\lambda}_{\text{dir}} \tag{18}$$

The limit tends towards $\alpha^{\lambda}_{\text{diff}}$ the more rough the surface or orography at the given grid point is. The weighting factor γ is parameterized as a function of the SSO standard deviation σ_{SSO} and the landuse class specific roughness length z_0. γ is close to 0 for landuse classes with 'smooth' vegetation/ orography and becomes 1 for $z_0 > 0.15\,\text{m}$ or $\sigma_{SSO} > 150\,\text{m}$.

$$\gamma = \max\left[0.01 \cdot (\sigma_{SSO} - 50), 10 \cdot (z_0 - 0.05)\right] \tag{19}$$

$$\gamma = \min(1, \max(0, \gamma)) \tag{20}$$

The functional dependency is depicted in Figure 5.

An example for 1st June 2012 04UTC, based on the diffuse albedos shown in Figure 1 and 2 is given in Figure 6.

References

Briegleb B, Ramanathan V. 1982. Spectral and diurnal variations in clear sky planetary albedo. *J. Appl. Meteorol.* **21**: 1160–1171.

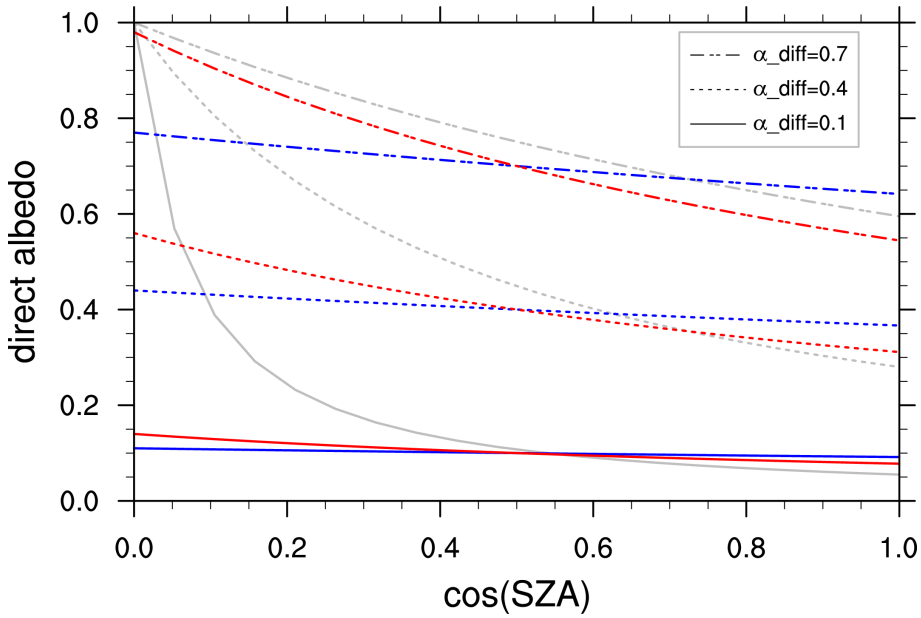

Figure 4: Solar zenith angle (SZA) dependence of the Black-sky (direct) albedo following Briegleb and Ramanathan (1982) (equation 15). Solid, dashed and long-dashed lines show the functional dependency for 3 different values of the diffuse albedo. Red lines show results assuming a strong ($d = 0.4$) functional dependency, while blue lines show results assuming a weak ($d = 0.1$) functional dependency. Grey lines show the Ritter-parameterization for comparison.

Schaaf CB, Gao F, Strahler AH, Lucht W, Li X, Tsang T, Tsang T, Strugnell NC, Zhang X, Jin Y, Muller J, Lewis P, Barnsley M, Hobson P, Disney M, Roberts G, Dunderdale M, Doll C, d'Entremont RP, Hu B, Liang S, Privette JL, Roy D. 2002. First operational brdf, albedo nadir reflectance products from modis. *Remote Sensing on Environment* **83**: 135–148.

Yang F, Mitchell K, Hou Y, Dai Y, Zeng X, Wang Z, Liang X. 2008. Dependence of land surface albedo on solar zenith angle: Observations and model parameterization. *Journal of Applied Meteorology and Climatology* **47**: 2963–2982.

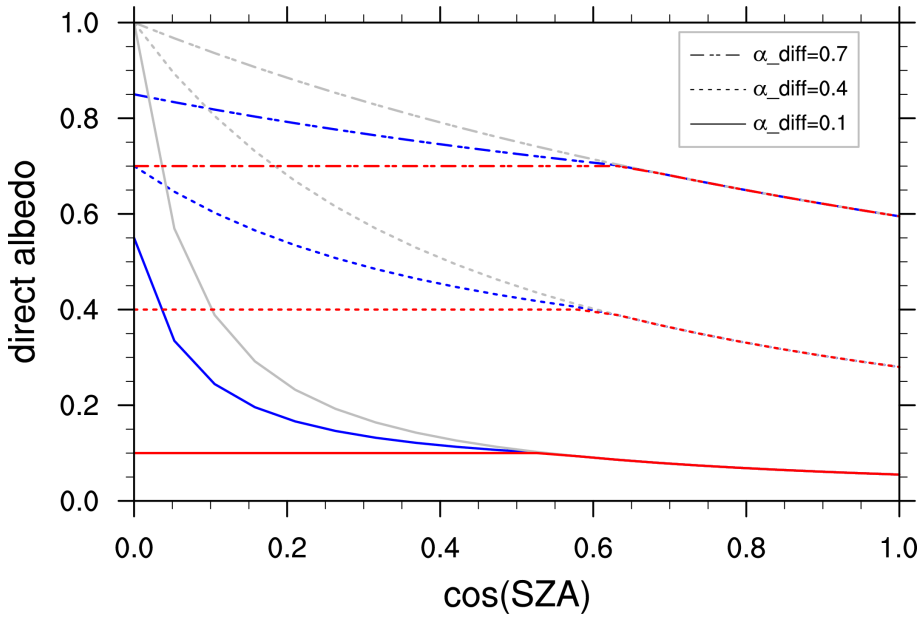

Figure 5: Solar zenith angle (SZA) dependence of the Black-sky (direct) albedo following Zängl, as it is currently used for snow-covered points. Solid, dashed and long-dashed lines show functional dependency for 3 different values of the diffuse albedo. Blue lines show results assuming a roughness length of $z_0 = 0.1$. Red lines are valid for $z_0 = 1.0$. For comparison the Ritter-Parameterization is shown in grey.

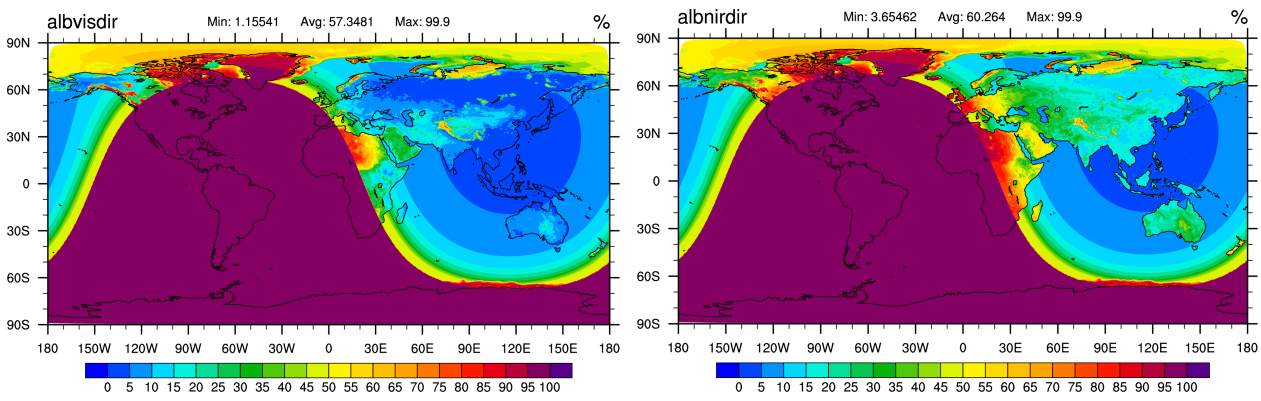

Figure 6: Black sky (direct) albedo for UV-visible (left) and near-infrared (right) spectral bands for the 4th Jan 2012 04UTC.